MICROEARTHQUAKE SEISMICITY ON THE DUKE RIVER, DENALI FAULT SYSTEM

M.A. Power
Department of Physics,
University of Alberta
Edmonton, Alberta
T6G 2E1

POWER, M.A., 1988. Microearthquake seismicity on the Duke River Fault, Denali Fault System: in Yukon Geology, Vol. 2; Exploration and Geological Services Division, Yukon, Indian and Northern Affairs Canada p. 61 - 68.

ABSTRACT

A seven station seismograph array operated at two sites on the western segment of the Duke River Fault between May 22, 1987 and August 13, 1987 detected 146 earthquakes of which 44 were located. Distribution of microearthquake epicentres, S-P times and moderate earthquake epicentres delineate three zones of seismicity. Most microseismicity is confined to a 15 km wide central zone, parallel to the Duke River Fault and centered approximately 5 km north of it, where shallow and midcrustal microearthquake focii are centered beneath structures deforming the Tertiary cover. Faulting here is well constrained to oblique thrusting on a slip plane striking parallel to the Cement Creek fault. A northern zone of shallow focus micro seismicity is centered on the Wolverine Plateau and the valley of the White River. A southern zone of microearthquake focii centred on the Icefield Ranges delineates an unmapped fault, 40 km long and striking west from known faults south of the Duke River Fault. The distribution of epicentres and a composite focal plane solution suggest that reverse faulting with southward vergence is occurring in this zone. The results of this study and the historical record of epicentres suggest that the Totschunda and Duke River Fault segments of the Denali Fault System are structurally linked and that no connection between the Denali Fault System and the Pacific margin is in this area.

RÉSUMÉ

En utilisant un réseau sismographique de sept stations dans deux sites du segment ouest de la faille de Duke River, entre le 22 mai 1987 et le 13 août 1987, on a pu déceler 146 séismes, et localiser 44 d'entre eux. La distribution des épicentres microsismiques, les temps de propagation des ondes S-P et la distribution d'épicentres de séismes d'intensité moyenne nous ont permis de délimiter trois zones de sismicité. La microsismicité est principalement limitée à une zone centrale de 15 km de large, parallèle à la faille de Duke River, centrée à environ 5 km au nord de celle-ci, et où des foyers microsismiques peu profonds et localisés dans la partie moyenne de la croûte sont centrés au-dessous de structures qui déforment la couverture tertiaire. A cet endroit, le faillage est bien limité à un charriage oblique qui s'est produit au-dessus d'un plan de glissement d'orientation parallèle à la faille de Cement Creek. Une zone microsismique septentrionale, avec foyer peu profond, est centrée sur le plateau Wolverine et dans la vallée de la rivière White. Une zone microsismique régionale, dont les foyers sont centrés sur les monts Icefield, délimite une faille non cartographiée de 40 km de long, de direction ouest à partir de failles connues situées au sud de la faille de Duke River. La distribution des épicentres et la résolution d'un plan focal composite suggèrent que dans cette zone, apparaissent des failles inverses caractérisées par une vergence sud. Les résultats de cette étude, et les enregistrements chronologiques des épicentres, suggèrent que les segments faillés de Totshunda et de Duke River qui appartiennent au réseau de failles de Denali sont liés du point de vue de leur structure, et qu'il n'existe aucun lien entre le réseau de failles de Denali et la marge pacifique dans cette région.

INTRODUCTION

Seismicity in the southwest Yukon Territory is generally restricted to two zones; one along the Pacific/North American plate boundary and the other straddling the Denali Fault System (Fig. 1) (Horner 1983). Earthquakes up to magnitude 8.6 have occurred at the plate boundary, where the Yakutat Block is actively accreting to the North American Plate along the Fairweather, Chugach-St. Elias and Border Ranges faults. The Dalton, Shakwak and Duke River segments of the Denali Fault System display a lower level of seismicity with recent earthquakes up to magnitude 6.5. Historically, the greatest number of small to moderate earthquakes has occurred on the Duke River Fault between the Duke River Depression and the Yukon/Alaska boundary. Displacement on the Denali Fault System is dominantly right-lateral (Campbell and Dodds 1978) but the western portion of the Duke River Fault has been mapped as transpressional bend across which crustal shortening is occurring (Plafker et. al., 1978). This report describes a survey of earthquake activity along this portion of the Duke River Fault during May - August 1987. Previous surveys of microseismicity along the Denali Fault System in the Yukon Territory were conducted by Boucher and Fitch (1969) and Horner (1983); neither were conducted in the area described in this paper.

FIELD PROCEDURE

An array of seven seismographs was installed and operated for 5-6 weeks at two locations shown in Figure 3. Sites A-G were located near Big Boundary Creek and operated from May 22, 1987 to July 2, 1987 and sites H-N were centered south of the confluence of St. Clare and Bull Creeks and operated from July 5, 1987 to August 13, 1987. The array consisted of 2 Sprengnether DR-100 and 2 Teledyne MCR digital event recorders and 3 Sprengnether MEQ-800 smoked paper drum seismographs; one MCR was configured with a vertical and pair of horizonatal seismometers, whereas the rest were equipped solely with vertical component seismometers. Digital event recorders are triggered by ground motion exceeding backround noise by a preset amplitude and record the 1.5 seconds of signal preceeding the trigger together with subsequent high amplitude ground motion whereas the drum seismographs provide a continuous record of ground motion. The array bandwidth was 29.75 Hz with a low cut at 0.25 Hz; individual instruments had wider response characteristics. Instrument gain varied between 66078 dB depending upon site conditions and the level of microseisms. Seismograph sites were serviced every 1-4 days and this schedule together with terrain conditions limited the size of the networks. To ensure accurate timing, 2 Benest Portable Precision Clocks were synchronized daily with WWV and

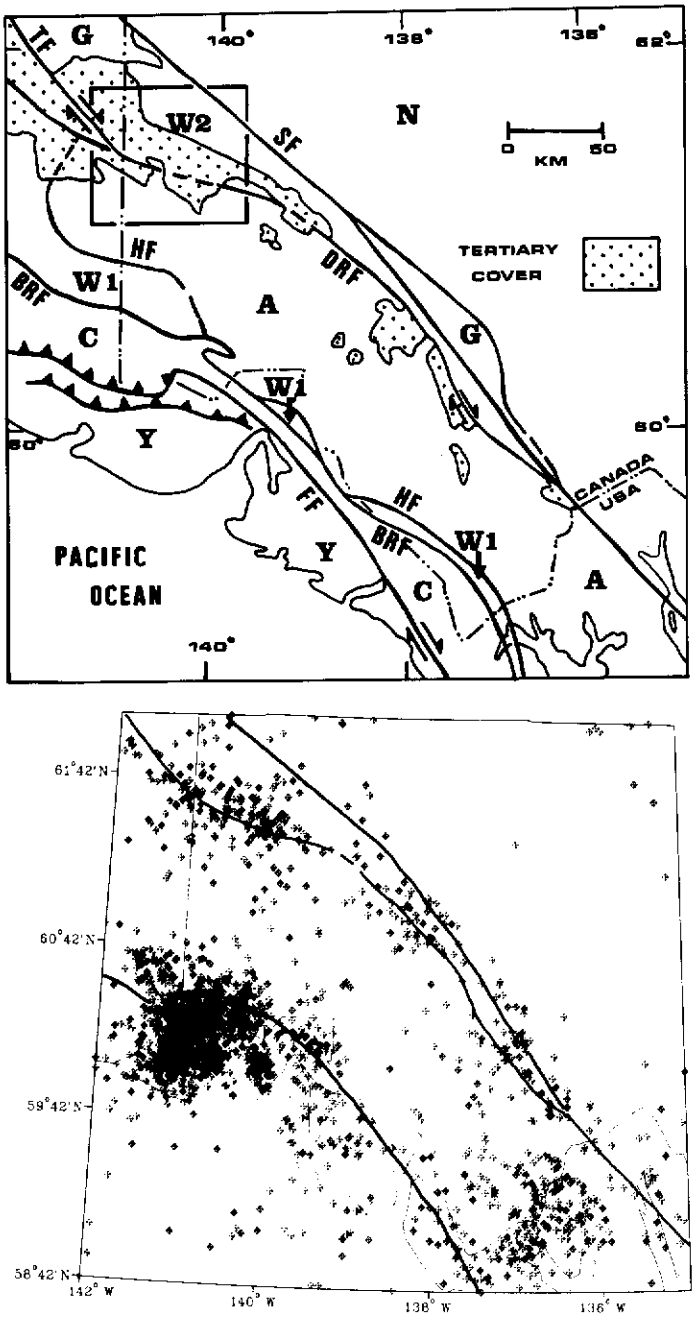

Figure 1. Tectonic elements and seismicity in the southwest Yukon Territory and southeastern Alaska (a) Principal faults and terrane distributions after Campbell and Dodds (1987). The study area is the rectangular region enclosed in the top left corner of the map. Symbols for elements of the Wrangell Terrane; W1 and W2, Alexander Terrane; A, Chugach Terrane; C, Yakutat Block, Y, in-board elements of the North American plate; N, Border Ranges Fault; BRF, Hubbard Fault, HF, Fairweather Fault; FF, Totschunda Fault; TF, Duke River Fault; DRF, Shakwak Fault; SF (b) Distribution of epicentres in the area of (a) from the Canadian Earthquake Catalogue superimposed on the traces of the Fairweather-Chugach- St. Elias Faults and the Denali Fault System.

in turn used to drift-correct seismograph clocks.

The smoked paper seismographs provided continuous coverage and produced the most useful records for the purpose of this study. Cool wet weather had a deleterious effect upon the performance of the digital event recorders by causing rapid battery deterioration and often large clock drifts. Limited tape and pre-event buffer capacity also restrict the usefulness of such instruments in reconnaissance studies: site noise or teleseismic earthquakes can fill tapes rapidly and emergent P-wave onsets from local earthquakes are often not recorded if the S-P separation exceeds the buffer capacity. Earthquakes located in this study were usually detected by three of the smoked paper instruments and by up to two of the digital event recorders.

DATA ANALYSIS

A total of 146 earthquakes were detected at one or more sites. Impulsive, high amplitude P- and S-wave arrivals were timed to within ± 0.05 s and ± 0.2 s respectively; arrivals of lesser quality had larger errors and were weighted accordingly. All arrivals were corrected for clock drift using double interpolation to correct for portable clock drift with respect to WWV and seismograph clock drift with respect to the portable clock. DR-100 and MEQ-800 seismograph clock drifts rarely exceeded 20 ms per day but MCR clock drift occasionally exceeded 100 ms per day and appeared to be disconcertingly non-linear. Arrivals detected at MCR sites were only used in solutions when their drift corrected arrival times were judged to be consistent with those recorded at surrounding stations.

Most earthquakes occurred outside of the detecting arrays and this created difficulty in determining focal coordinates. Least-squares methods are usually applied to the earthquake location problem and often fail to converge to an acceptable solution when an event is outside of an array or when no site is closer to the epicentre than the focal depth (Lee and Stewart 1981). A method was devised to eliminate origin time as an explicit variable and thus permit a more stable geometric search for a solution. It is fully described in Power (1988) and is summarized here.

Consider an array of n stations at which P and S arrivals t_{Pk} and t_{Sk} [k= 0, 1, 2...n] are recorded. For a trial focus and origin time, theoretical arrival times t^*_{Pk} and t^*_{Sk} may be calculated. The difference in trial and recorded arrival times between stations i and j denoted as $t_{ij}=t_i-t_j$, the difference in theoretical recorded S-P separations for any station i (t_{SPi} and t^*_{SPi}) and weighting factors for each recorded arrival (w_{pi}, w_{si}) may be used to define a time-difference residual.

$$\tau=\sqrt{\frac{1}{2}\sum_{i=1}^{n}\sum_{j=1}^{n}\left\{w_{p_i}w_{p_j}\left(t_{p_{ij}}-t^*_{p_{ij}}\right)^2+w_{s_i}w_{s_j}\left(t_{s_{ij}}-t^*_{s_{ij}}\right)^2\right\}+\sum_{i=1}^{n}w_{p_i}w_{s_i}\left(t_{SP_i}-t^*_{SP_i}\right)^2} \qquad (1)$$

This form of residual depends only on the geometry of the incoming body wave with terms in the summation affected to various degrees by the azimuth, radial distance and depth of focus. S-P separations were incorporated into the residual to restrain the search to the region surrounding the global minimum; tests with real data showed that in cases where the distribution of arrival times differs from that expeced in simple layered velocity models, the location algorithm tends to search for a best-fit plane wave solution (ie. a solution at infinity).

Since these residuals are solely a function of spatial coordinates, geometric search techniques may be applied to the earthquake location problem. We found that the combination of a geometric search to locate the general area of the global minimum and a modified conjugate gradient search to pinpoint it works satisfactorily. The geometric search consists of evaluating the time-difference residual at the corners and centre of a rectangular volume, selecting the minimum and reconstructing a reduced search volume about this point. The initial volume has dimensions of 100 x 100 x 30 km and the process is repeated until the search volume has contracted to a cube of 0.001 km^3. This generally locates a search point near the global minimum. From this point, a parallel tangents search is initiated to determine a solution. A suitable search cutoff value can be determined by substituting the sum of absolute timing errors for the arrival time differences in equation (1). Origin times are back calculated using the average of the recorded P-wave arrival times less the travel times from focus to the array stations.

This location algorithm was tested using synthetic data (Fig. 2). Two sets of 36 earthquakes at epicentral distances of 20 and 40 km and focal depths of 0-30 km were located by a 10 km wide tripartite array with a constrast in station elevation of 1.0 km. The earthquakes were distributed at 10°intervals on the circles shown in Figure

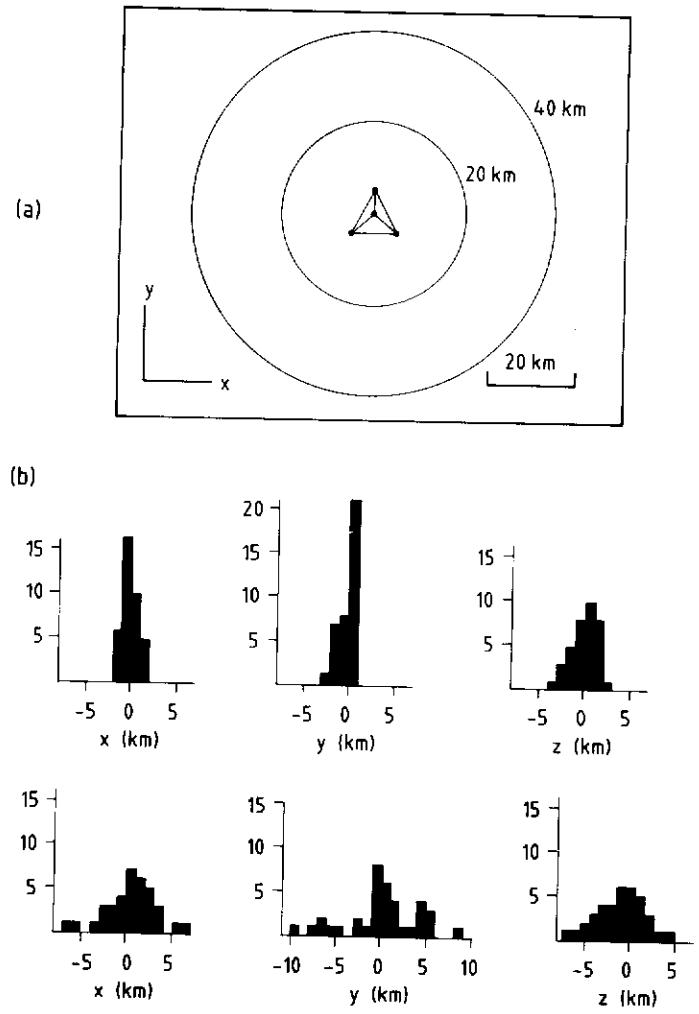

Figure 2. Test of the time-difference residual method using earthquakes in a half-space velocity model and a 10 km wide tripartite array. (a) Array configuration showing coordinate axes (positive z is down). Test earthquakes with epicentres 20 km and 40 km from the centre of the array are located at 10° intervals on the circles. (b) Histograms of error in focal coordinates. Error in focal coordinates for the set of earthquakes 20 km from the centre of the array are shown on the top row and for the set 40 km from the centre of the array on the bottom row.

2(a) and their P and S wave arrival times, rounded to ± 0.01 s, were calculated using a half-space velocity model (V_p=6.0 km/s, V_s= 3.5 km/s). The location algorithm was then tested by locating the earthquakes using the arrival times and velocity model as input. Histograms of error in the determination of focal coordinates are shown in Figure 2(b). This test was performed without the addition of S-P separations into the residual calculation. Such a modification improves convergence behavior when dealing with real arrival times and will probably further reduce the location error; additional tests are being conducted. A plane of symmetry parallel to the yz-plane through the centre of the array accounts for the rapid deterioration in the determination of the y-coordinate with increasing epicentral distance; no such plane of symmetry exists in the field arrays.

The earthquakes detected in this study were located using the velocity model determined by Stephens et al. (1984). This minimized residuals in a limited test data set and is probably the best regional velocity model available. Focal coordinates of earthquakes more than 2 array widths from the centre of the detecting array are considered accurate to ± 5 km while focal coordinates of events nearer the arrays are probably accurate to ± 3 km. A number of events had focal depths restrained to 5.0 km but this did not significantly alter their epicentral coordinates.

RESULTS

Focal coordinates and time-difference residuals of earthquakes detected in this study are tabulated in Table 1 and displayed together with geological structures in Figure 3. Most events are located near the Duke River Fault and structures associated with it. Very little activity was detected near the Totschunda Fault but this may be a consequence of the distance of the arrays from this feature. The Duke River Fault, in the cental portion of the map area, juxtaposes the Mesozoic and older Wrangellia Terrane against the Alexander Terrane and is overlain by deformed calc-alkalic volcanic rocks (Neogene Wrangell Lavas). The Tertiary rocks are most intensely deformed

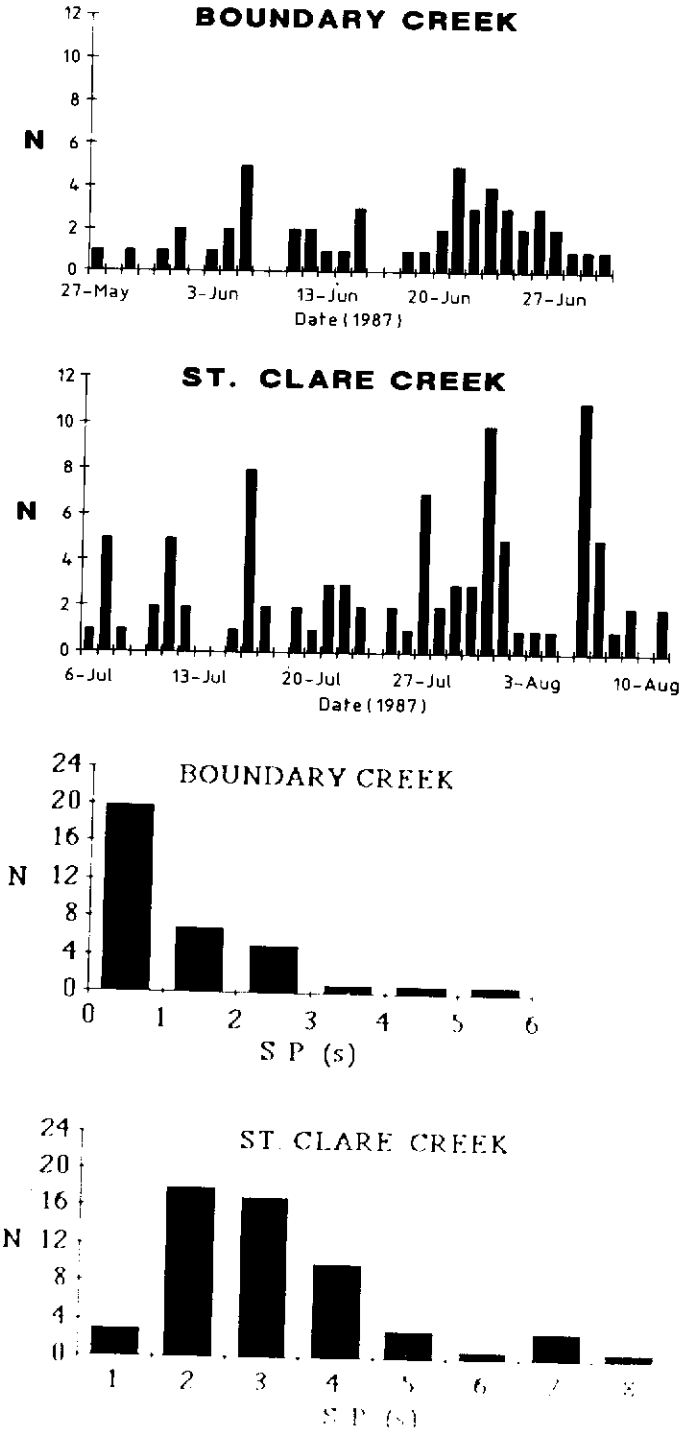

Figure 4. Histograms of S-P separation and daily earthquake frequency. (a) Histograms of S-P separations for unlocated earthquakes are both arrays. N is the number of events. (b) Daily frequency of earthquakes at both arrays. All events are included.

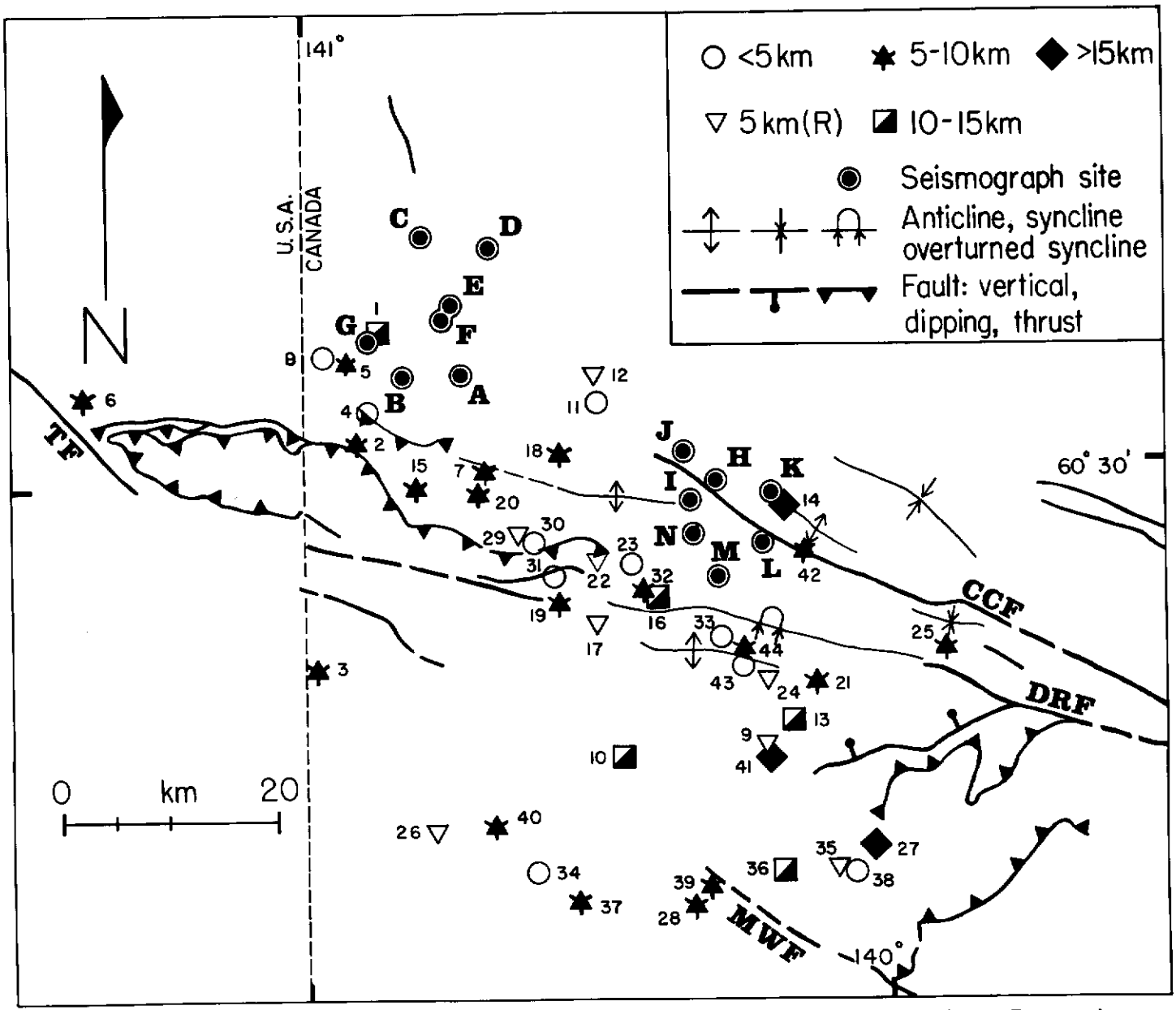

Figure 3. Seismograph sites, microearthquake epicentres coded for focal depth and geological structure in the study area. Event numbers correspond to those in Table 1. Symbols include: TF- Totschunda Fault, DRF- Duke River Fault, CCF- Cement Creek Fault, MWF- Mount Wood Fault. Geology after Campbell and Dodds (1982) and MacKevett (1978).

in a wide zone astride the exposed and buried trace of the Duke River Fault and most of the detected seismicity occurs there.

A number of events are located in the Icefield Ranges, a rugged region south of the Duke River Fault where extensive glaciers limit geological mapping. Ten events on July 31 and August 6, 1987 define a slightly curved band of seismicity which originates near mapped faults south of the Duke River Fault and extends to the west for 40 km, cutting across the inferred trace of the Mt. Wood Fault (Campbell and Dodds 1987). North of the Duke River Fault and its associated structures, a small number of earthquakes were located beneath the Wolverine Plateau and the valley of the White River, a low lying region covered by undisturbed Quaternary surficial deposits.

All but three of the located earthquakes had focal depths less than 15 km. Event 41 was an isolated earthquake detected nearly simultaneously at sites H, J, K and N which yielded a focal depth of 36 km. No deep focus events have been detected in this area by the regional network (R. Horner 1987, personal communication) but earthquakes at this depth have been detected beneath Quaternary volcanoes 100 km west of this site (Stephens et al., 1984).

The paucity of earthquakes north of the Duke River Fault is partially the result of instrument problems encountered during the operation of the Boundary Creek array. Figure 4(a) is a histogram of S-P separations for unlocated events detected at both arrays. The large number of events with S-P separations of 0-1 s recorded at Boundary Creek indicate that significant shallow earthquake activity occurs beneath the valley of the White River. The pattern of S-P separation recorded at the St. Clare Creek array is consistent with the distribution of earthquakes recorded there; most are 10-30 km from the array along the length of the Duke River Fault.

The temporal pattern of earthquakes is characterized by bursts of seismicity (Fig. 4(b)). The sequences recorded on July 31 and August 6, 1987 define the 40 km long trend of seismicity beneath the Icefield Ranges and occurred between 09:11 and 09:16 hrs (UTC) on July 31 and between 14:14 and 14:29 hrs on August 6, 1987. During July and August episodes of increased activity recurred every 4-6 days.

The epicentral distributions and geological structure suggest that the study area can be subdivided into 3 domains (Fig. 5): (1) the northern domain, centered on the Wolverine Plateau and the valley of the White River and characterized by relatively shallow seismicity, (2) the central domain straddling the Duke River Fault and its

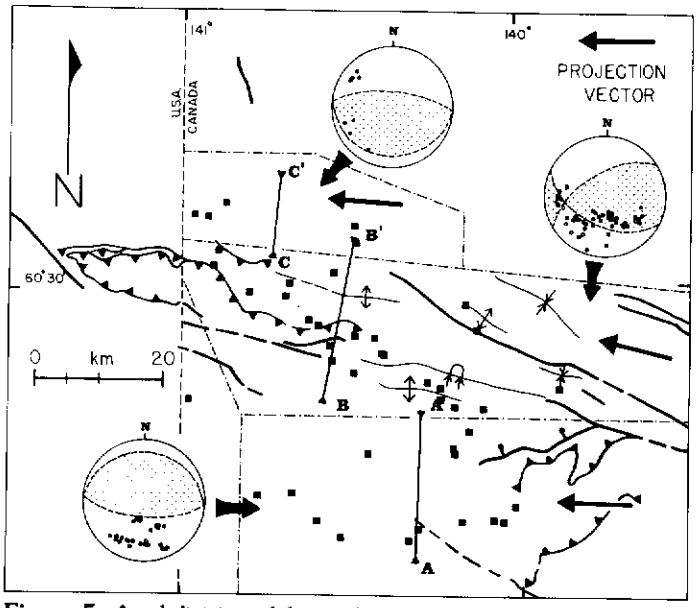

Figure 5. A subdivision of the study area based on microseismicity and geological structure. A-A', B-B' and C-C' are the traces of vertical projection planes in the south, central and north microseismicity zones. Focii are projected into the projection planes along the horizontal vectors shown in each domain. Equal area projections of first motions prepared using events with focal depths less than 15 km show compressions as filled circles and compressional quadrants with stippling.

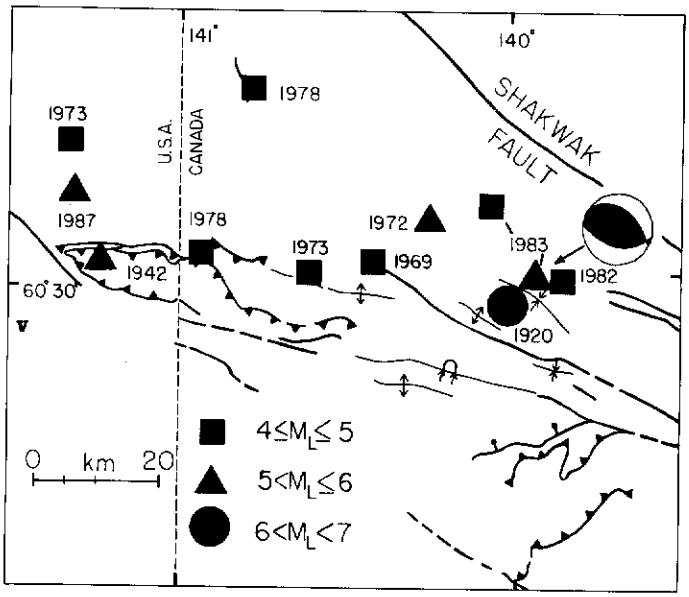

Figure 7. Epicentres of earthquake with local magnitudes greater than 4.0 from the Canadian Earthquake Catalogue.

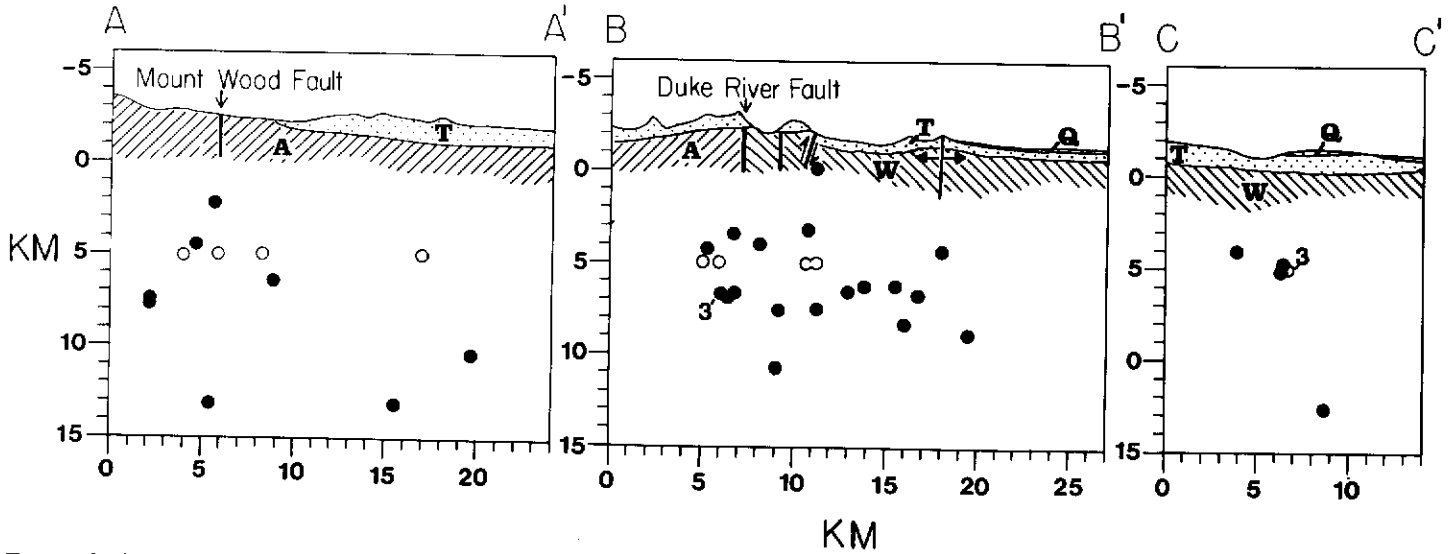

Figure 6. Cross-sections showing projections of earthquake focii into the planes of section together with the structural geology along the line of section. Lines of section correspond to those in Figure 5 and open circles designate earthquakes restricted to focal depths of 5.0 km. A- Alexander Terrane W- Wrangellia Terrane, T- Tertiary cover rocks (Wrangell Lavas), Q- Quarternary surficial deposits.

associated structures and (3) the southern domain, centered on the Icefield Ranges.

Axial traces of major faults and folds are essentially parallel in the central domain, suggesting that the relationship between earthquake focii and geological structures may be clarified by projecting hypocentres up or down a vector parallel to the structural trend. This procedure was performed using TRIPOD (Charlesworth et al., 1987) for focii in all 3 domains, horizontal projection vectors parallel to the mountain front separating the north and central domains in the north domain, the mean structural trend in the central domain, and the mean trend of the July 31/August 6, 1987 earthquake sequence in the south domain. Lines of section and projection vectors are indicated in Figure 5 and the sections are shown in Figure 6. The trend of the projection vector in the central domain could arguably be varied by ± 5° but the distribution of focii would not be seriously altered since most are near the projection plane.

No conclusive results can be inferred from projections in the north and south domains; the association between earthquake focii and the Mt. Wood Fault is coincidental. In the central domain, seismicity is concentrated beneath the Duke River Fault and structures north of it in a zone approximately 15 km wide. Earthquakes in this domain are well located and the distribution of focii suggests a complex zone of disruption rather than a single fault or set of discrete faults in the subsurface.

Equal-area projections of the first motions and preferred composite focal plane solutions for the three domains are shown in Figure 5. Solutions involving pure strike or dip slip may be constructed for data in the north domain; the arbitrary solution shown was con-

structed by restraining the strike of nodal planes to the trend of the mountain front separating the north and central domains. First motions from 21 earthquakes in the central domain constrain a unique solution with oblique thrusting along either 147° 30° (hanging wall up) or 25° 40° (hanging wall up). Eight of the 50 first motions are inconsistent with this solution but 6 of these are very close to the focal planes and are thus probably subject to reading errors. The southwest-dipping nodal plane conains the first of the two displacement vectors, strikes parallel to the trace of Cement Creek Fault (Skulski and Francis 1986) and the axial traces of a number of minor folds associated with it, and seems to be the most probable slip plane. Antithetic faulting are common in the map area although a splay from the Duke River Fault 10 km west of site M seems appropriately oriented. Thus slip on the other nodal plane cannot be ruled out. In the south domain, the first motion pattern is more complex with 7 compressions evenly distributed amongst 23 dilatations. The dominant first motion is dilatational and the preferred solution was constructed by setting the strike of the nodal planes parallel to the trend of the July 31, 1987 and August 6, 1987 earthquake sequences. This solution is non-unique but other solutions involving substantial components of strike slip will produce nodal planes which are oblique to the traces of mapped faults and to the trend of the earthquake sequences. This suggests that oblique thrusting or reverse faulting probably is occurring here. Campbell and Dodds (1982) have mapped a fault with unspecified displacement dipping steeply to the north and a thrust fault cutting a small pocket of Wrangell Lavas in the northeast corner of this domain. The orientation and vergence of these two faults suggests that any current displacement will be to the south.

THE HISTORICAL RECORD

Figure 7 shows the distribution of earthquakes, with local (Richter) magnitudes greater than 4.0 in the Canadian Earthquake Catalogue, superimposed on the geological structure in the study area. Horner (1983) stated that earthquakes occurring prior to 1965 are probably located to ± 50 km whereas more recent events are considered accurate to ± 25 km. Complete coverage down to magnitude 5.0 and 4.0 dates from the 1950's and 1971. Despite limitations in the historical record, the prevalence of moderate earthquakes north of the Duke River Fault and the absence of seismicity on the Shakwak Fault north of its divergence from the Duke River Fault are apparent. Even if the 1920 earthquake occurred on the Shakwak Fault, the complete record indicates relative quiescence on this feature (see Fig. 1(b)). The pattern of moderate earthquake seismicity on the Duke River Fault resembles the pattern of microseismicity; most activity is confined to the area immediately north of the Duke River Fault with some earthquakes of moderate magnitude occurring beneath the Wolverine Plateau and the valley of the White River. A catalogue of focal plane solutions for these earthquakes would be useful. A solution prepared by Alaskan Geophysical Institute for the 1983 M_L = 5.0 earthquake beneath the Wolverine Plateau indicated thrust faulting along a southwest dipping nodal plane (Alaska Geophysical Institute 1984). Given the absence of any vertical faults in the north domain, the prevalence of compressional features in the central zone and the transpressional nature of the regional tectonic setting, oblique thrusting is probably the most prevalent failure mechanism.

POSSIBLE EVIDENCE FOR HOLOCENE TECTONISM

No geomorphological evidence of Holocene displacement on the Duke River Fault or any of its subsidiary faults is evident in airphotographs (Clague 1979), while up to 146 m of dominantly right-lateral displacment has occurred on the Totschunda Fault (Plafker et al., 1977). Till and alluvial deposits adjacent to the Cement Creek (near site H - Fig. 3) dated as "Pliocene and (?) Pleistocene" by Campbell and Dodds (1982) show evidence of tectonic disturbance (C. Dodds 1987, personal communications, Souther and Stanciu 1976). Where exposed at Bull Creek, the succession is uniformly tilted 20° to the southwest (Figure 8). These deposits appear to be Late Wisconsin (S. Morison 1987), personal communication) and thus are essentially part of a blanket of Quaternary surficial deposits covering most of the low lying area north of the Duke River Fault. Tilting does not seem to have resulted from glacial tectonism; the section at Bull Creek shows no evidence of internal disruption in a 400 m section extending from the valley floor to the top of the adjacent ridge.

CONCLUSIONS

Microearthquake activity near the Duke River Fault defines 3

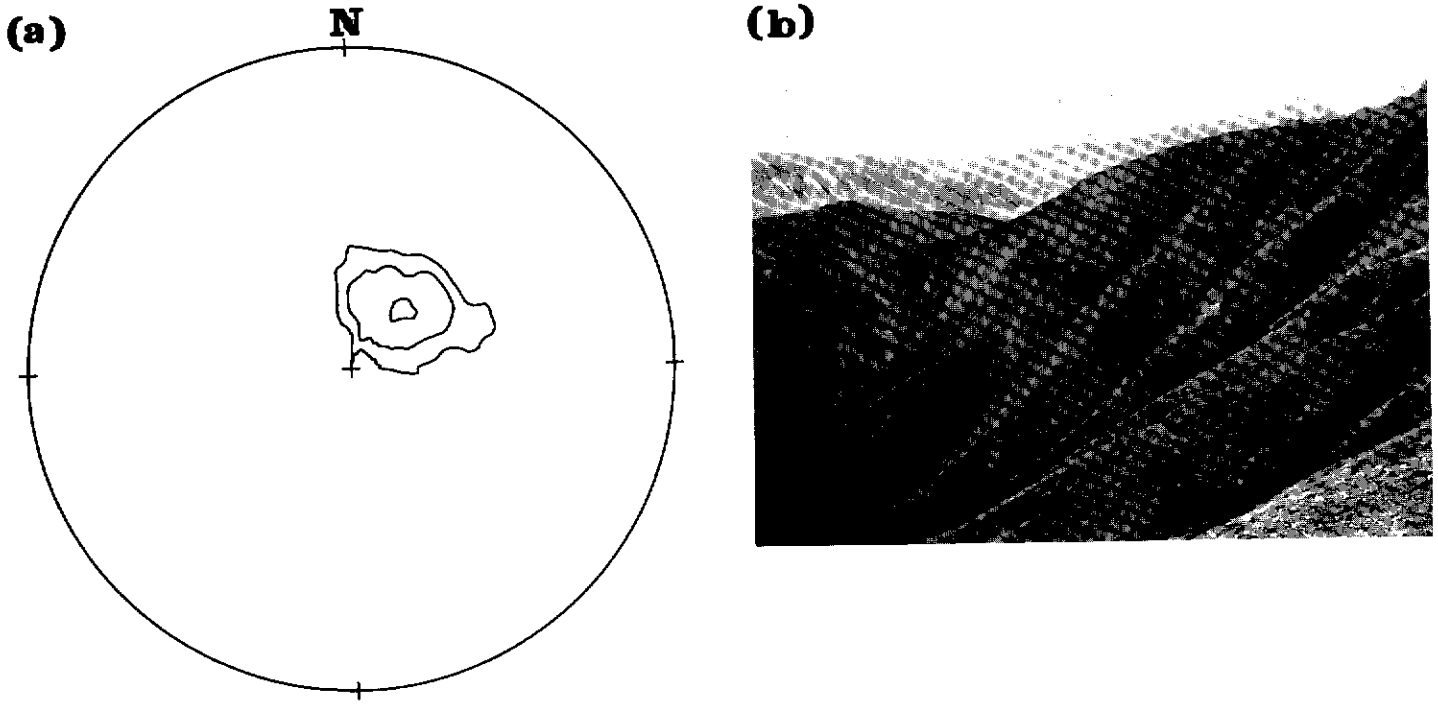

Figure 8. Tectonically disturbed tills and fluvial deposits at Bull Creek. (a) Equal area projection of poles to bedding measured from the base to the top of the exposed section. Contours denote 5% 20% and 50% of 28 poles in a 1% counting circle. The mean pole to bedding (first eigenvalue of the distribution of orientations) is 38.7° 70.1°. (b) Photograph of the uppermost part of the till unit 200 m north of site H.

zones of seismicity which are related to known structures and the pattern of moderate earthquake epicentres. Most seismicity occurs in a central zone straddling the Duke River Fault and structures north of it. The complex pattern of focii observed in projections parallel to the trend of the local structure suggests that a wide zone of faulting exists beneath structures in the deformed Tertiary cover. Shallow seismicity occurs beneath low lying areas north of the Duke River and Cement Creek faults and a number of moderate earthquakes have been reliably located in this zone. A southern zone, centered on the Icefield Ranges, is characterized by a low level of microseismicity, by crustal shortening along high angle reverse faults or thrust faults and by an absence of moderate earthquake activity. The July 31 and August 6, 1987 earthquake sequences appear to have resulted from failure along a single discrete structure; the two bursts of seismicity (3 events in 5 minutes on July 31 and 7 events in 15 minutes on August 6, 1987) define a simple curved trend originating near the traces of known faults. First motions and the trend of the structure in relation to the local stress field strongly suggest that it is either a thrust fault or high angle reverse fault. Both possibilities are consistent with faults observed on the eastern end of the trend.

Microearthquake activity in the central zone constrains a focal plane solution consistent with local structure and the regional tectonic setting. Displacement on the Totschunda Fault is dominantly horizontal and its mean trend (-140°) differs by approximately 7° from that of the displacement vector in the central zone (147°). The trend of the central zone displacement vector and the mean trend of the Duke River Fault (-285°) differ by approximately 42° suggesting that nearly equal components of dextral displacement and crustal shortening characterize the local tectonic regime. The overall pattern of earthquake activity suggests that the deformation front has migrated north from the Duke River Fault. Tilted surfical deposits at Bull Creek may provide evidence of Holocene tectonism but this hinges on definitive dating. Holocene compression and the concomitant folding or thrust faulting of strata north of the Duke River Fault are consistent with the observed pattern of microseismicity and moderate earthquake activity in this area.

Recent models for Holocene tectonics in the Gulf of Alaska involve a connecting transform fault between the Totschunda and Fairweather faults through the St. Elias Mountains (eg. Lahr and Plafker 1980, Richter and Matson 1971). The data summarized in this report suggest that no such connection exists; faulting in the southern zone cuts across the inferred trend of this transform at a high angle, no microearthquake activity was observed at the southern end of the Totschunda Fault and no firm evidence of such a connecting fault exists in the regional record of epicentres (Figure 1(b)). The discrepancy between displacements on the Duke River and Totschunda segments of the Denali Fault System may be resolved if large, predominantly dextral strike-slip displacements on the Totschunda Fault and small oblique displacements along faults in a wide zone parallel to the Duke River Fault are equivalent.

ACKNOWLEDGMENTS

This work was supported by grants from the Boreal Institute for Northern Studies, by logistical support from the Exploration and Geological Services Division of Indian and Northern Affairs Canada in Whitehorse, Y.T. and by funds from the Natural Sciences and Engineering Research Council. Drs. R. Ellis (University of British Columbia) and D. Bingham (Alberta Environment) are thanked for generously loaning seismographs and ancillary equipment to the field party. The author profited from discussions with R. Horner, C. Dodds, P. Erdmer and L. Tober. E. Nyland advised the author throughout this work and reviewed this paper. The author extends special thanks to Wilf Kruggel for his capable and cheerful assistance in the field.

REFERENCES

BOUCHER, G. and FITCH, T.J., 1969. Microearthquake seismicity of the Denali Fault; Journal of Geophysical Research, Vol. 74, p. 638-6648.

CAMPBELL, R.B. and DODDS, C.J., 1978. Operation Saint Elias, Yukon Territory; Geological Survey of Canada, Paper 78-1A, p. 35-41.

CAMPBELL, R.B. and DODDS, C.J., 1982. S.W. Kluane Lake Map Area (115 G and F (E 1/2); Geological Survey of Canada; Open File 829.

CAMPBELL, R.B. and DODDS, C.J., 1987. Structural elements, terrane distributions and cover rock sequences, Saint Elias Mountains (unpublished).

CLAGUE, J.J., 1979. The Denali Fault System southwest Yukon Territory - A geologic hazard; in Geological Survey of Canada, Paper 79-1A, p. 169-178.

CHARLESWORTH, H.A.K., GOLD, C., WYNNE, D. and GUIDOS, J., 1987. TRIPOD 2.1, A microcomputer-based system for collecting, storing, retrieving and processing structural, stratigraphic and positional data from outcrops and drillholes; University of Alberta, Edmonton: Department of Geology, 70 p.

GEOPHYSICAL INSTITUTE OF ALASKA - FAIRBANKS, 1984. Biennial report 1983-84.

HORNER, R., 1983. Seismicity in the St. Elias region of northwestern Canada and southeastern Alaska; Bulletin of the Seismological Society of America, Vol. 73, No. 4, p. 1117-1137.

LAHR, J.C. and PLAFKER, G., 1980. Holocene Pacific-North American plate interactions in southern Alaska: implications for the Yakataga Seismic Gap; Geology Vol. 8, p. 483-486.

LEE, W.K.H. and STEWART, S.W., 1981. Principles and applications of microearthquake networks; Advances in Geophysics, Supplement 2, Academic Press.

MACKEVETT, E.M.Jr., 1978. Geologic map of the McCarthy quadrangle; United States Geological Survey, Miscellaneous Inventory Series, Map I-1032.

PLAFKER, G., HUDSON, T. and RICHTER, D.H., 1977. Preliminary observations on late Cenozoic displacements along the Totschunda and Denali Fault Systems; United States Geological Survey, Circular 733, p. 67-69.

PLAFKER, G., HUDSON, T. and BRUNS, T., 1978. Late Quaternary offsets along the Fairweather Fault and crustal plate interactions in southern Alaska; Canadian Journal of Earth Sciences, Vol. 15, p. 805-816.

POWER, M.A., 1988. Seismicity and neotectonics of the Duke River Fault, Yukon Territory; Unpublished M.Sc. Thesis, University of Alberta, (in prep.).

RICHTER, D.H. and MATSON, N.A.Jr., 1971. Quaternary faulting in the Eastern Alaska Range; Geological Society of America Bulletin, Vol. 82, p. 1529-1540.

SKULSKI, T. and FRANCIS, D., 1986. On the geology of the Tertiary Wrangell Lavas in the St. Clare Province, St. Elias Mountains, Yukon Territory; Yukon Geology 1984, Vol. I, p. 161-170.

STEPHENS, C.D., FOGLEMAN, K.A., LAHR, J.C. and PAGE, R.A., 1984. Wrangell Benioff zone, southern Alaska, Geology Vol. 12, No. 6, p. 373-376.

Table 1. Microearthquake coordinates and residuals.

Event	Date	Time (UTC)	UTM	X (km)	Y (km)	Z (km)	Residual	n-m
1	June 7, 1987	10:19:56.7	EU	6.86	31.56	12.69	0.00	0
2	June 12, 1987	13:04:27.9	EU	4.95	21.62	6.21	1.56	2
3	June 12, 1987	18:04:58.9	EU	1.16	0.60	7.91	1.18	1
4	June 25, 1987	00:38:40.5	EU	5.70	24.00	4.33	0.55	1
5	June 25, 1987	16:35:08.7	EU	4.09	29.4	5.24	1.10	1
6	June 29, 1987	09:08:37.9	DU 79.61	25.85	8.06	0.63	0	
7	June 30, 1987	09:01:26.3	EU	16.86	18.93	8.32	0.04	0
8	June 31, 1987	18:11:39.7	EU	1.98	29.69	4.81	0.59	3
9	July 17, 1987	01:58:52.6	ET	42.87	93.25	5.00(R)	1.62	2
10	July 21, 1987	05:06:45.0	ET	29.53	92.25	13.15	1.82	2
11	July 22, 1987	12:00:08.8	EU	27.35	25.36	4.10	0.75	2
12	July 22, 1987	12:01:49.5	EU	27.06	28.10	5.00(R)	0.74	2
13	July 27, 1987	08:06:44.7	ET	45.40	95.84	10.43	0.82	2
14	July 27, 1987	08:11:15.8	EU	44.62	15.76	20.72	0.57	1
15	July 27, 1987	10:22:06.5	EU	10.59	17.47	6.55	1.44	1
16	July 27, 1987	23:31:36.8	EU	31.95	7.71	10.73	0.50	1
17	July 28, 1987	14:48:10.2	EU	27.17	4.89	5.00(R)	0.59	1
18	July 29, 1987	12:04:02.0	EU	23.82	20.63	8.89	0.74	1
19	July 29, 1987	17:40:45.6	EU	23.72	6.80	6.69	0.25	2
20	July 29, 1987	23:19:35.8	EU	16.25	16.88	6.25	0.30	0
21	July 30, 1987	18:14:49.3	ET	47.58	99.45	6.58	1.89	3
22	July 30, 1987	18:15:25.2	EU	27.28	10.65	5.00(R)	0.86	1
23	July 30, 1987	23:38:29.4	EU	30.41	10.37	-0.31	1.10	1
24	July 31, 1987	08:34:57.0	ET	43.01	99.71	500(R)	0.38	1
25	July 31, 1987	09:10:33.8	EU	59.58	2.60	7.50	3.20	3
26	July 31, 1987	09:11:35.7	ET	12.20	85.6	5.00(R)	1.10	1
27	July 31, 1987	09:12:21.9	ET	52.88	84.09	17.31	0.51	1
28	July 31, 1987	09:16:09.9	ET	36.06	78.62	7.75	1.15	2
29	July 31, 1987	13:09:50.5	EU	19.92	13.17	5.00(R)	1.11	2
30	August 1, 1987	15:53:57.7	EU	21.44	12.29	3.21	0.67	1
31	August 1, 1987	15:24:39.8	EU	23.38	9.08	4.00	1.14	1
32	August 1, 1987	18:58:39.5	EU	31.56	7.94	7.56	0.24	0
33	August 2, 1987	03:13:08.2	EU	38.72	3.50	3.45	0.59	1
34	August 6, 1987	14:14:39.4	ET	21.51	81.64	4.47	0.59	2
35	August 6, 1987	14:15:01.5	ET	49.49	81.90	5.00(R)	0.24	1
36	August 6, 1987	14:15:40.7	ET	44.44	81.64	13.14	1.30	1
37	August 6, 1987	14:16:05.8	ET	25.34	79.02	7.42	0.85	2
38	August 6, 1987	14:16:34.9	ET	51.09	81.64	2.23	0.88	1
39	August 6, 1987	14:17:58.7	ET	37.51	80.4	5.07	0.96	2
40	August 6, 1987	14:29:41.1	ET	17.59	85.99	6.40	2.80	2
41	August 7, 1987	09:39:20.3	ET	43.17	92.34	36.64	0.96	2
42	August 7, 1987	21:07:16.8	EU	46.49	11.77	6.73	1.51	2
43	August 11, 1987	05:23:36.1	EU	40.73	0.81	4.26	0.86	1
44	August 12, 1987	05:47:12.2	EU	40.8	2.61	6.89	0.51	1